CSIRO PUBLISHING

Exploration Geophysics
http://dx.doi.org/10.1071/EG16136

Comparative analyses of seismic site conditions and microzonation of the major cities in Gangwon Province, Korea

Abid Ali[1] Ki Young Kim[1,2]

[1]Department of Geophysics, College of Natural Sciences, Kangwon National University, Chuncheon 24341, Korea.
[2]Corresponding author. Email: kykim@kangwon.ac.kr

Abstract. To determine the seismic site conditions and microzonation of Chuncheon, Wonju and Gangneung cities in the Gangwon Province, Korea, the dispersion curves of Rayleigh waves were derived at 313 sites by the extended spatial autocorrelation (ESPAC) method. Using the shear-wave velocities (*Vs*) determined from dispersion curves, average depth to the bedrock (D_b) and *Vs* at the top of the bedrock (Vs_b), the overburden layer (Vs_o) and the top 30 m depth layer (Vs_{30}) were determined. The resonance frequencies (f_r) were then computed using both D_b and Vs_o. The estimated averages of the three cities were 13 ± 7 m for D_b, 472 ± 109 m/s for Vs_b, 248 ± 44 m/s for Vs_o, 411 ± 157 m/s for Vs_{30} and 5.8 ± 2.8 Hz for f_r. Microzonation maps based on the proxy-based Vs_{30} indicated that the three cities were mainly categorised into National Earthquake Hazards Reduction Program (NEHRP) classes B, C and D, with a minor proportion of A. Although no area was estimated to be in class E using the proxy-based Vs_{30}, the Vs_{30} values derived from the recorded Rayleigh waves at 13 sites in Gangneung were less than 180 m/s. This indicates a greater vulnerability to seismic amplification during large earthquakes in this city, which had the smallest Vs_o, Vs_{30} and f_r, and the greatest D_b of the three cities. Microzonation maps, together with information for f_r, can be effectively used for seismic risk assessments, urban planning, and disaster management.

Key words: microzonation, Rayleigh wave, seismic amplification, seismic site condition, Vs_{30}.

Received 8 November 2016, accepted 14 November 2016, published online 9 December 2016
Originally submitted to KSEG 11 May 2016, accepted 12 October 2016

Introduction

Site conditions play a significant role in the scale of ground shaking and the extent of earthquake damage. The thickness (average depth to bedrock, D_b) and shear-wave velocity (*Vs*) of an unconsolidated soil column overlying bedrock provides essential information about the response of a site to large ground movements. The soft sediments in the soil layer can drastically modify the amplitude and frequency of propagating seismic waves. Large human populations that settle in low-altitude areas predominantly covered by alluvium and fluvial deposits are at risk of severe human and economic damage due to substantial site amplification and nonlinear effects resulting in soil liquefaction. Therefore, determining the D_b and *Vs* of the unconsolidated soil column overlying bedrock could contribute important information to seismic hazard assessments (Steidl, 2000).

Seismic site conditions can be mapped using the average *Vs* of the top 30 m (Vs_{30}) (Borcherdt, 1994). Vs_{30} has been a key parameter used to define site effects and soil amplification since the first implementation of the Uniform Building Code recommendations and the provisions of the National Earthquake Hazard Reduction Program (NEHRP) from the USA (ICC, 1997; BSSC, 1997). Later, the Vs_{30} was advocated as a predictive criterion for site amplification by many reliable organisations, including the Building Seismic Safety Council (BSSC, 2003), International Building Codes (ICC, 2000, 2003) and the Korean Seismic Design Standard (MOCT, 1997). During the last few decades, several environmentally friendly and cost-effective geophysical techniques have been developed to evaluate the *Vs* of near-surface sediments, particularly the top 30 m. Often Vs_{30} is evaluated indirectly in broad areas using appropriate proxies. Among such proxies, topographic slope (Wald and Allen, 2007; Allen and Wald, 2009; Thompson and Wald, 2012), elevation (Chiou et al., 2008), local geology (Romero and Rix, 2001; Wills and Clahan, 2006; Scasserra et al., 2009), geomorphologic factors (e.g. convexity and texture) and geotechnical site information (Chiou et al., 2008; Seyhan et al., 2014) are commonly used.

The Korean Peninsula (KP) lies in a region of low to moderate seismicity in the Far East, where the Pacific, Philippine and Eurasian plates meet. In recent years, seismic activity has increased in the KP, particularly in Gangwon Province that lies in the eastern Korean seismic zone (Figure 1; Houng and Hong, 2013; Chiu and Kim, 2004). A few moderate seismic events, such as the Uljin ($M_W = 5.1$; Kang and Baag, 2004) and Odaesan ($M_L = 4.5$; Jo and Baag, 2007) earthquakes have been triggered in the seismic zone in recent times. The inland areas of the KP consist of plains, valleys, hills and mountains, which are covered with soils of widely varying thickness, formed from weathering and fluvial activity. These residual soil columns could result in a large amount of ground shaking during strong seismic activity. More than 50% of the total population of Gangwon Province dwells in the Chuncheon, Wonju and Gangneung cities (KOSIS, 2015). The ground surfaces of these cities primarily consist of forests, agricultural land and downtown areas (Figure 1; KME, 2014). Most inhabitants live in the downtown and agricultural areas.

To analyse the seismic site conditions of these three major cities and microzonate them, we compiled previous passive

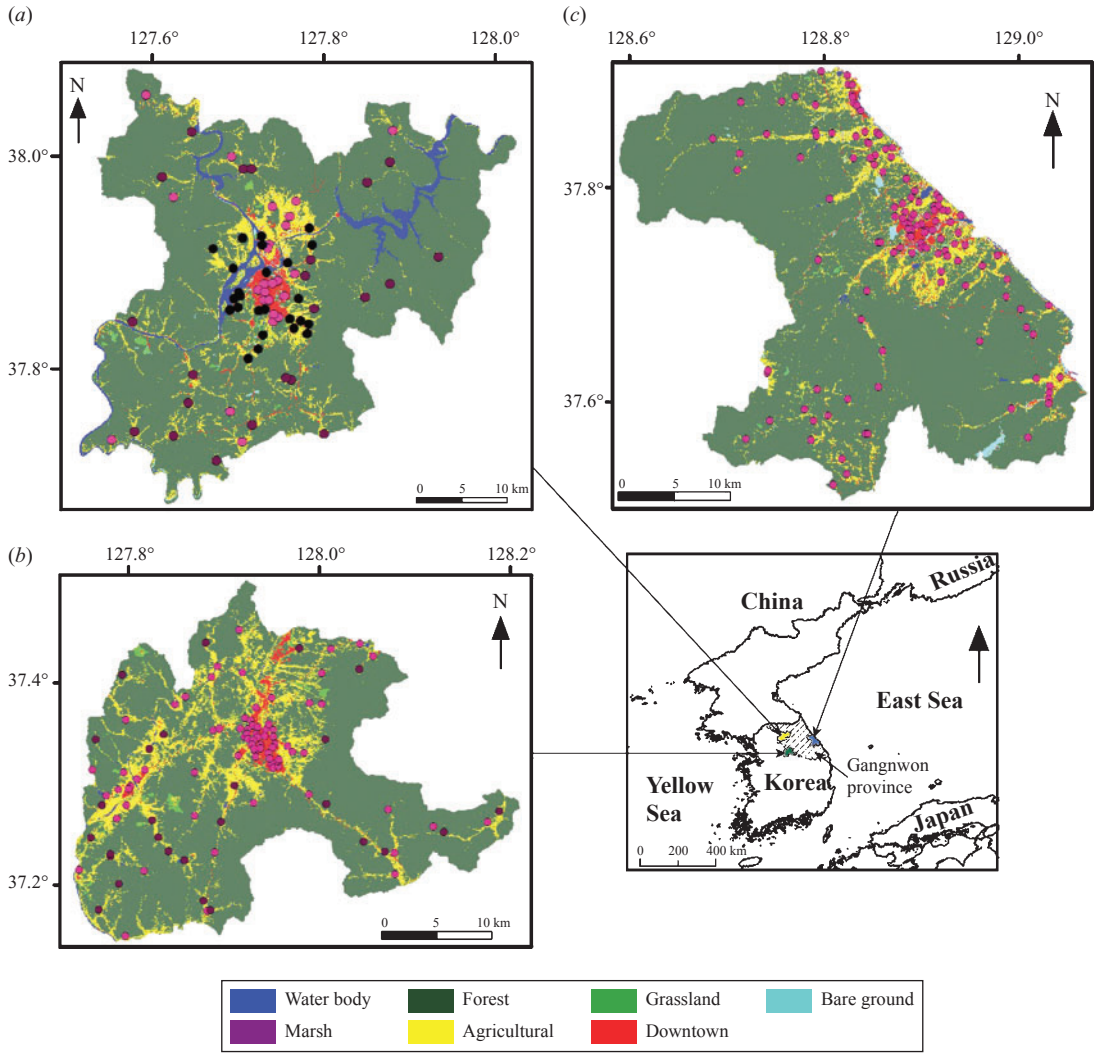

Fig. 1. Locations of previous (pink and black circles) and new (dark purple circles) recording sites in (*a*) Chuncheon, (*b*) Wonju and (*c*) Gangneung cities of the Gangwon Province (hatched area), Korea, superimposed on land cover maps. The solid black circles denote the locations where passive seismic data were recorded for 5 min using four 1 Hz portable seismographs.

and active surface-wave data (Jung and Kim, 2014; Kim et al., 2014; Ali and Kim, 2016), and recorded additional data to enhance data quality and spatial coverage. From the one-dimensional (1D) *Vs* profiles determined from the dispersion curves of Rayleigh waves, average depths to the soft bedrock (D_b) and the *Vs* at the top of the bedrock (Vs_b), we obtained the overburden layer (Vs_o) and Vs_{30}, as well as the resonance frequency (f_r). Then, seismic microzonation maps were constructed based on the Vs_{30} estimated using topographic proxies for each city. Finally, we compared the estimated values between the three cities as well as other cities or regions in the world with different topographic and geologic conditions in order to validate the applied method and analysis results.

Methodology

The *Vs* of shallow geologic layers is generally determined by conventional exploration seismic methods and laboratory tests. To minimise environmental issues and budgetary constraints, we applied the extended spatial autocorrelation (ESPAC) method to obtain the dispersion curves of Rayleigh waves contained in active and passive seismic data (Okada, 2003). The spatial autocorrelation (SPAC) method has a fundamental advantage over the f-k method, because it extracts seismic energy propagating across the entire array without considering the noise direction and the presence of single or multiple energy sources (Asten, 2006).

Microtremors are considered stochastic and stationary phenomena both in space and time, and can be presented as a summation of the angular frequencies ω that arrive independently from multiple directions (Aki, 1957). These signals are a function of time, station separation r, and the orientation θ of the recording positions. The wave energy contained in microtremors that propagate with a unique velocity at a given frequency can be defined by the SPAC coefficient $\rho(\omega, r)$, which is the spatially averaged coherency of an omnidirectional plane wave recorded at a single pair of receiver locations:

$$\rho(\omega, r) = \frac{1}{2\pi}\int_0^{2\pi} exp\{(irk\cos(\theta - \varphi)\}d\theta, \qquad (1)$$

where φ and k are the azimuth of the plane wave and angular wave number, respectively. Because the right side of Equation 1 is a Bessel function of the first kind of zero order, $J_0(rk)$, the power spectra of microtremors at a particular station are used to obtain the plane-wave velocities. Because k relates to phase velocity $J_0(rk)$ such that $k = \frac{\omega}{c(\omega)}$, the propagation velocity of Rayleigh waves can be expressed by the SPAC coefficient:

$$\rho(\omega, r) = J_0\left(\frac{\omega r}{c(\omega)}\right). \quad (2)$$

Vs profiles were estimated from the dispersion curves of Rayleigh waves recorded using the ESPAC (Ling and Okada, 1993) method to facilitate data acquisition and avoid limitations due to array size. In the ESPAC method, no restrictions are imposed on the geometry of the array, so that seismic data recorded at different times using a different array size and receiver spacing can be jointly used to derive the SPAC coefficient in Equation 2.

To obtain a 1D *Vs* structure from the phase-velocity dispersion curves of Rayleigh waves for a layered-earth model, various inversion schemes have been attempted (Thomson, 1950; Haskell, 1953; Aki, 1957; Schwab, 1970). The phase velocity $c(\omega)$ is expressed in a nonlinear implicit form as a function of the subsurface parameters, including the number of layers (N), P-wave velocity (v_p), S-wave velocity (v_s), density (ρ) and thickness (h) of each layer, as follows:

$$c_j = c(\omega_j; v_{p1}, v_{s1}, \rho_1, h_1, \ldots\ldots, v_{pN}, v_{sN}, \rho_N, h_N), \quad (3)$$

where subscript j denotes the discrete frequency for the phase velocity. To derive a *Vs* model from $c(\omega)$, Equation 3 is expanded using Taylor's Series and eliminating the higher-order terms from the equation. The difference between observed and estimated $c(\omega)$ for a model can be approximated by a first-order partial differential equation. The difference Δc_J between the observed and estimated $c(\omega)$ for the j^{th} frequency in an N-layered model is expressed as:

$$\Delta c_j = \sum_{i=1}^{N}\left[\frac{\partial c_i}{\partial v_{pi}}\cdot\frac{\partial v_{pi}}{\partial v_{si}} + \frac{\partial c_j}{\partial v_{si}} + \frac{\partial c_j}{\partial \rho_i}\cdot\frac{\partial \rho_i}{\partial v_{si}}\right]\Delta v_{si}\; j = 1, 2, \ldots..M. \quad (4)$$

Phase velocities are computed for the M discrete frequencies for which the least-squares solution is required. To reduce the number of unknowns, Equation 4 needs to be constrained by setting a constant thickness of each layer, and assuming both v_{pi} and ρ_i as functions of v_{si} before the inversion (Xia et al., 1999; Okada, 2003). The damped least-squares method, which is a fast and stable iterative inversion scheme, was used to solve Equation 4 (Marquardt, 1963).

Data acquisition and processing

Previous data

In Chuncheon, passive and active surface waves were recorded using 1 Hz velocity sensors and 4.5 Hz vertical geophones from January 2011 to May 2013 (Figure 1*a*; Jung and Kim, 2014). At 25 sites, passive seismic data were recorded on four portable seismographs for 300 s at a sample rate of 250 Hz using the ESPAC configuration (Okada, 2003). In the field, one sensor was placed at the centre and the other three were positioned on the circumference of concentric circles, with radii of 5, 10, 20 and 40 m (Figure 1*a*). At 27 sites, including two replicated locations, both passive and active seismic signals were acquired for 2 or 8 s at a sample rate of 1000 or 500 Hz using the vertical geophones and a 24-channel engineering seismometer. The geophones were laid out in a linear or L-shaped array, with receiver intervals of 2 to 5 m.

The 4.5 Hz vertical geophones, recorder and receiver configurations used for Chuncheon city were also used to record passive and active seismic data at 78 sites in Wonju city in 2013 (Figure 1*b*; Kim et al., 2014) and 136 sites in Gangneung city in 2014 (Figure 1*c*; Ali and Kim, 2016). The geophone intervals were 2 to 4 m in Wonju and 3 to 5 m in Gangneung. The optimal geophone intervals were chosen at each site based on the ground condition and security of the minimum penetration depth of 40 m.

Additional surveys

The spatial coverage of previous recordings was not dense enough to define the near-surface characteristics of shallow geologic layers in Chuncheon and Wonju, particularly in mountainous regions. Hence, to increase the spatial coverage and improve the images of the Rayleigh-wave dispersion curves, additional recordings were performed at 22 sites in Chuncheon and 27 sites in Wonju from November 2014 to January 2015 (Figure 1*a*, *b*). More than half of the additional sites were located at elevations of 150 m or higher to cover the sparsely sampled mountain regions, while the remaining 23 sites were located in low-altitude areas with lower sample densities. Both active and passive data were recorded at each station using the same acquisition equipment and configuration as the previous surveys (Jung and Kim, 2014; Kim et al., 2014).

Data processing

The ESPAC method was used to determine the phase velocities of Rayleigh waves in both the 264 previous and 49 newly acquired records. Among the 313 sites, both passive and active data were available at 239 sites, for which SPAC coefficients were independently computed in the frequency range of 0–60 Hz using Equation 2. Then the dispersion images were combined to enhance signal-to-noise ratios, improve resolution, and make it easier to distinguish the fundamental mode from the higher modes of Rayleigh waves. At the remaining 74 sites, only passive data were used to obtain dispersion images. Dispersion curves of the fundamental mode were determined on smoothed velocity spectra yielded after the calculation of 3-point moving averages.

The *Vs* profiles were retrieved from the phase-velocity dispersion curves using the damped least-squares inversion method as described in the methodology section. For initial models, *Vs* values were set at 1.1 times the phase velocities of Rayleigh waves and depths were set as one-third of the corresponding wavelengths (Hayashi et al., 2006). The previous inversion models for sites in Chuncheon and Wonju consisted of 40 layers of 1 m thickness (Jung and Kim, 2014; Kim et. al., 2014). However, to generate *Vs* models for the sites in Gangneung, the number and thickness of layers were fixed at 20 and 2 m, respectively (Ali and Kim, 2016). We used the same parameters as those used in the Gangneung area to obtain *Vs* models for all three cities. The final *Vs* models were obtained by iteratively modifying the inversion models more than 20 times, which reduced the root-mean-square (RMS) errors to less than 5%.

From the 313 1D *Vs* profiles in the three cities, the D_b, Vs_b, Vs_o, f_r and Vs_{30} were determined, after which the values of D_b, Vs_b and Vs_o were verified through comparisons with 573 geologic logs (KRC, 2014; MOLIT, 2014; Figure 1), three P-wave profiles (Kim et al., 2015), two SH-wave refractions (Jung and Kim, 2014; Kim et al., 2014) and three multichannel analyses of surface waves (MASW) (Kim et al., 2015).

Results and discussion

Depth to bedrock (D_b)

Vs values were derived from the active and passive surface-wave methods to define D_b in the three cities. The bedrock in these cities predominantly consist of Precambrian gneiss and

schist and Mesozoic granite and granodiorite. The *Vs* ranges of 'soft bedrock' and 'engineering bedrock' have been defined as 400–700 m/s (Keçeli, 2012; Ali and Kim, 2016) and 700–1500 m/s (Ansal and Tönük, 2007), respectively. Accordingly, we used these *Vs* ranges to demarcate the soft bedrock boundaries (Ali and Kim, 2016). The soft bedrock is comprised mostly of moderately weathered rock ($360 \leq Vs \leq 540$ m/s), but can also include soft rock ($Vs \geq 680$ m/s; Sun et al., 2015).

From the seismic data recorded at 313 recording sites, only 277 *Vs* profiles with a maximum inverted *Vs* of 400 m/s or greater were incorporated to compute D_b. At 71 out of 72 recording sites in Chuncheon, the estimated average D_b ($\overline{D_b}$) was 12 ± 5 m. This updated value is 20% less than the previous estimation by Jung and Kim (2014), mainly because additional recordings were made at sparsely sampled high-altitude areas where D_b is generally shallow (Table 1; Ali, 2016). The $\overline{D_b}$ were estimated to be 11 ± 5, 15 ± 4, 9 ± 3 and 21 ± 8 m in the agricultural, downtown, forest and bare ground areas, respectively. In Wonju, the $\overline{D_b}$ was determined to be 13 ± 6 m from the 105 *Vs* profiles, which is 19% less than the previous estimate (Kim et al., 2014). The estimated $\overline{D_b}$ values for the agricultural, downtown and forest areas in this city were 11 ± 6, 15 ± 6 and 8 ± 3 m, respectively (Table 1). The $\overline{D_b}$ in Gangneung was previously estimated to be 15 ± 9 m (Ali and Kim, 2016), whereas here the estimated $\overline{D_b}$ values for the agricultural, downtown and forest areas were 19 ± 11, 16 ± 4 and 13 ± 8 m, respectively (Table 1). Overall, the $\overline{D_b}$ was estimated to be 13 ± 7 m in the three major cities in Gangwon Province. With regard to land cover, the estimated $\overline{D_b}$ values were 13 ± 8, 15 ± 5, 11 ± 7 and 21 ± 8 m in the agricultural, downtown, forest and bare ground areas, respectively.

The probability distribution curves of D_b values (Figure 2*a*) clearly show that Gangneung ($\overline{D_b} = 15 \pm 9$ m) has deeper bedrocks than Chuncheon ($\overline{D_b} = 12 \pm 6$ m) and Wonju ($\overline{D_b} = 13 \pm 6$ m). The thicker overburden layers in Gangneung indicate a greater susceptibility to seismic amplification as recently proposed by Ali and Kim (2016). Greater D_b values were estimated in the downtown areas than in the agricultural and forest areas in all three cities. The presence of thick overburden layers in the downtown areas indicated a possible exposure of the local population to fatal levels of ground shaking during large earthquakes. In contrast, most forest areas with low D_b values were considered relatively safe from ground amplification.

Compared to the mode D_b value of 15 m for weathered rock depths previously determined from 183 *in-situ* seismic tests in Korea (Sun et al., 2012), the estimated $\overline{D_b}$ values in this study were slightly lower. However, the $\overline{D_b}$ recorded here are greater than the average depth of 10 m for the shale bedrock in western Sydney, Australia, determined using the MASW method (Tokeshi et al., 2013). Our estimates of D_b were also greater than the 0.7 to 11.7 m values reported in Olathe, United States, using the MASW method (Miller et al., 1999) and 5 to 15 m in Ottawa, Canada (Pugin et al., 2013), determined by SH-wave reflection profiling. Our estimates were in agreement with the $\overline{D_b}$ of 12 ± 11 m for weathered rocks composed of granite, metasediments and gneisses ($Vs = 360$ m/s; Anbazhagan et al., 2013) in Australia, China and India using surface-wave methods. Although our estimates of D_b are within a reasonable range, direct comparisons with D_b values estimated in other regions may be misleading because definitions of lithology and of bedrock (based on the *Vs* gradient) may not be the same as ours.

Vs of overburden (Vs_o)

The overburden layers in the Chuncheon, Wonju and Gangneung cities are predominantly composed of Quaternary alluvium and fluvial terrace deposits (Lee et al., 1974; Park et al., 1989; Kihm and Hwang, 2011). The overburden layer includes fill, fluvial soil and weathered soil formed as a result of chemical or physical weathering of the mother rock in the study areas. The estimated average *Vs* values for the soft overburden layer ($\overline{Vs_o}$) in Chuncheon and Wonju were 252 ± 46 and 247 ± 46 m/s, respectively (Table 1), which are 12 and 15% less than the previous estimates (Jung and Kim, 2014; Kim et al., 2014). The updated $\overline{Vs_o}$ values were lowest in bare ground areas (225 ± 12 m/s), followed by agricultural (246 ± 47 m/s), downtown (260 ± 41 m/s) and forest (269 ± 49 m/s) areas in Chuncheon. Except for the sites in forest areas, where D_b values were lowest, the estimated $\overline{Vs_o}$ values were less than 265 m/s. The updated $\overline{Vs_o}$ in the agricultural, downtown and forest areas in Wonju were 242 ± 48, 253 ± 42 and 245 ± 51 m/s, respectively. The $\overline{Vs_o}$ was previously estimated to be 247 ± 40 m/s in Gangneung (Ali and Kim, 2016), where the estimated $\overline{Vs_o}$ values were 234 ± 41, 253 ± 36 and 252 ± 39 m/s for the agricultural, downtown and forest areas, respectively. The overall $\overline{Vs_o}$ for the three cities was 248 ± 44 m/s. With regard to surface cover, the $\overline{Vs_o}$ estimates were 242 ± 46, 254 ± 40, 253 ± 43 and 225 ± 12 m/s for the agricultural, downtown, forest and bare ground areas, respectively. The Vs_o lognormal distribution curves (Figure 2*b*) reveal that the probability of lower Vs_o values in Gangneung ($\overline{Vs_o} = 247 \pm 40$ m/s) is higher than in Chuncheon ($\overline{Vs_o} = 252 \pm 50$ m/s) and Wonju ($\overline{Vs_o} = 247 \pm 47$ m/s).

The estimated $\overline{Vs_o}$ values were consistent with estimations in Bangalore, India ($\overline{Vs_o} = 259 \pm 41$ m/s; Anbazhagan and Sitharam, 2009), but slightly less than the average *Vs* of 280 m/s previously determined for alluvial soil in Korea by Sun et al. (2012). This small disagreement may be due to the differences in the methodology used, lithology and the sparse sampling regimes adopted in other studies.

Vs of bedrock (Vs_b)

The updated average *Vs* was estimated to be 478 ± 108 m/s for the Precambrian and Mesozoic bedrocks ($\overline{Vs_b}$) in Chuncheon, which was 7% less than the previous estimate by Jung and Kim (2014). In the agricultural, downtown, forest and bare ground areas, the newly estimated $\overline{Vs_b}$ values were 451 ± 60, 426 ± 26, 633 ± 152 and 421 ± 6 m/s, respectively. In Wonju, the overall updated $\overline{Vs_b}$ of 459 ± 77 m/s was 20% less than the previous estimate (Kim et al., 2014). This major enhancement was accomplished by both supplementary recording in sparsely sampled areas and careful reprocessing, including the improved determination of dispersion curves and their inversion for *Vs* in both cities. The newly derived $\overline{Vs_b}$ values were 473 ± 90, 444 ± 63 and 464 ± 71 m/s in the agricultural, downtown and forest areas, respectively. In Gangneung, the $\overline{Vs_b}$ was estimated to be 482 ± 134 m/s in our previous study (Ali and Kim, 2016). The $\overline{Vs_b}$ values were 463 ± 145, 437 ± 29 and 507 ± 145 m/s in the agricultural, downtown and forest areas, respectively. The overall $\overline{Vs_b}$ values for all three cities was estimated to be 472 ± 109 m/s. With regard to land cover, the $\overline{Vs_b}$ values were estimated to be 462 ± 98, 439 ± 52, 518 ± 144 and 421 ± 6 m/s in the agricultural, downtown, forest and bare ground areas, respectively. The Vs_b lognormal probability distribution curves (Figure 2*c*) show that many sites in Wonju ($\overline{Vs_b} = 459 \pm 65$ m/s) have lower Vs_b values than Chuncheon ($\overline{Vs_b} = 477 \pm 91$ m/s) and Gangneung ($\overline{Vs_b} = 480 \pm 98$ m/s).

Table 1. Summary of the depth to the bedrock (D_b), Vs of the bedrock (Vs_b), Vs of the overburden (Vs_o), average Vs to the upper 30 m depth (Vs_{30}) and resonance frequency (f_r) in the major cities in Gangwon Province, Korea.

'*Ns*' and 'μ' represent the number of recording sites incorporated for computation and the corresponding average value, respectively.

Study area	Land cover	D_b (m)				Vs_b (m/s)				Vs_o (m/s)				Vs_{30} (m/s)				f_r (Hz)			
		Ns	Min	Max	μ	*Ns*	Min	Max	μ	*Ns*	Min	Max	μ	*Ns*	Min	Max	μ	*Ns*	Min	Max	μ
Chuncheon	Agricultural	41	4	24	11	41	400	676	451	41	109	330	246	42	234	950	447	41	2.6	13.0	6.4
	Downtown	13	8	22	15	13	402	486	426	13	195	339	260	13	281	592	388	13	2.7	7.1	4.7
	Forest	13	4	12	9	13	415	935	633	13	181	352	269	13	485	927	642	13	5.3	12.9	8.4
	Bare ground	4	14	30	21	4	414	427	421	4	208	237	225	4	233	338	287	4	1.9	4.2	3.0
	Overall	71	4	30	12	71	400	935	478	71	109	352	252	72	233	950	462	71	1.9	13.0	6.3
Wonju	Agricultural	44	6	36	11	44	401	804	473	44	142	350	242	44	246	837	449	44	1.8	13.5	6.3
	Downtown	45	6	28	15	45	403	813	444	45	161	369	253	45	256	698	390	45	2.4	14.0	4.8
	Forest	16	4	14	8	16	404	633	464	16	142	355	245	16	385	696	528	16	5.0	11.2	7.7
	Overall	105	4	36	13	105	401	813	459	105	142	369	247	105	246	837	436	105	1.8	14.0	5.9
Gangneung	Agricultural	29	4	42	19	29	403	1190	463	28	143	344	234	41	131	946	302	28	1.2	10.9	4.0
	Downtown	18	8	24	16	18	407	489	437	18	208	322	253	29	166	561	314	18	2.2	10.1	4.3
	Forest	54	4	42	13	54	403	1230	507	53	188	325	252	66	142	869	424	53	1.3	12.0	6.4
	Overall	101	4	42	15	101	403	1230	482	99	143	344	247	136	131	946	364	99	1.2	12.0	5.4
Overall	Agricultural	114	4	42	13	114	400	1190	462	113	109	350	242	127	131	950	401	113	1.2	13.5	5.8
	Downtown	76	6	28	15	76	402	813	439	76	161	369	254	87	166	698	364	76	2.2	14.0	4.7
	Forest	83	4	42	11	83	403	1230	518	82	142	355	253	95	142	927	471	82	1.3	12.9	7.0
	Bare ground	4	14	30	21	4	414	427	421	4	208	237	225	4	233	338	287	4	1.9	4.2	3.0
	Overall	277	4	42	13	277	400	1230	472	275	109	369	248	313	131	950	411	275	1.2	14.0	5.8

The $\overline{Vs_b}$ values determined in this study for the three cities were much less than the 650 m/s previously determined for weathered rocks in Korea by Sun et al. (2012). However, our estimated $\overline{Vs_b}$ values were greater than estimates obtained in many other locations, including Ottawa, Canada ($\overline{Vs_b}$ = 140 m/s; Pugin et al., 2013); Olathe, Kansas, United States ($\overline{Vs_b}$ = 244 m/s; Miller et al., 1999); and Bangalore, India ($\overline{Vs_b}$ = 330 m/s; Anbazhagan and Sitharam, 2009). The new estimate of $\overline{Vs_b}$ was also greater than the threshold Vs of 300 m/s for the engineering bedrock in Japan (Annaka et al., 1997; IISEE, 2016). Similar to the case of $\overline{Vs_o}$, the discrepancy with the results in Sun et al. (2012) may have arisen from the difference in the methodology used, lithology and the definition of bedrock.

Resonance frequency (f_r)

To determine the resonance and fundamental frequencies of a site, several geophysical methods, including soil-to-rock spectral ratios (Borcherdt, 1970), horizontal-to-vertical spectral ratios (Nakamura, 1988; Lermo and Chávez-García, 1993) and generalised inversions (Iwata and Irikura, 1988; Boatwright et al., 1991), are often applied. In this study, the site responses of the three major cities were determined based on the f_r derived from the Vs profiles at each site using the following relationship (Haskell, 1960):

$$f_r = \frac{Vs_o}{4D_b}, \tag{5}$$

For the computation of f_r using Equation 5, we used the values of Vs_o and D_b at 71, 105 and 99 sites in Chuncheon, Wonju and Gangneung, respectively. The inverse relationships between f_r and D_b indicated in Equation 5 were evident on the f_r–D_b plots (Figure 4*a*). The correlation coefficients (r) were 0.85, 0.82 and 0.95 for Chuncheon, Wonju, and Gangneung, respectively, for the constrained power regression of:

$$f_r = \alpha D_b^{-1}, \tag{6}$$

where α is a quarter of Vs_o. Using the values of 59.49, 59.13 and 63.73 m/s for α in Equation 6, $\overline{Vs_o}$ was calculated to be 238, 237 and 255 m/s for Chuncheon, Wonju and Gangneung, respectively. Compared to the previous estimations of $\overline{Vs_o}$ obtained from the inverted Vs profiles, the errors were less than 6%. Both the small errors in $\overline{Vs_o}$ and the large r values of the regression analyses may verify our results for Vs_o and D_b derived from the 1D Vs profiles.

Next, the computed f_r values were used to evaluate seismic site responses according to the type of land cover (Table 1). In Chuncheon, the computed f_r varies from 1.9 to 13.0 Hz, with an average of 6.3 ± 2.7 Hz (Figure 3*a*). Here, the lowest average f_r ($\overline{f_r}$) was observed at 3.0 ± 1.1 Hz in bare ground, followed by the downtown (4.7 ± 1.5 Hz), agricultural (6.4 ± 2.7 Hz) and forest (8.4 ± 2.4 Hz) areas. In Wonju, the f_r values were in the range of 1.8–14.0 Hz, with an average of 5.9 ± 2.6 Hz (Figure 3*b*). In the agricultural, downtown and forest areas of the city, the $\overline{f_r}$ values were 6.3 ± 2.7, 4.8 ± 2.4 and 7.7 ± 1.6 Hz, respectively. In Gangneung, the overall $\overline{f_r}$ was previously calculated to be 5.4 ± 2.9 Hz (Figure 3*c*; Ali and Kim, 2016). Here, the estimated $\overline{f_r}$ values were 4.0 ± 2.4, 4.3 ± 1.8 and 6.4 ± 3.1 Hz in the agricultural, downtown and forest areas, respectively. Overall, the $\overline{f_r}$ was 5.8 ± 2.8 Hz for all three cities. With regard to land cover, the $\overline{f_r}$ values were 5.8 ± 2.8, 4.7 ± 2.1, 7.0 ± 2.9 and 3.0 ± 1.1 Hz in the agricultural, downtown, forest and bare ground areas, respectively. The f_r lognormal probability distribution curves (Figure 2*d*)

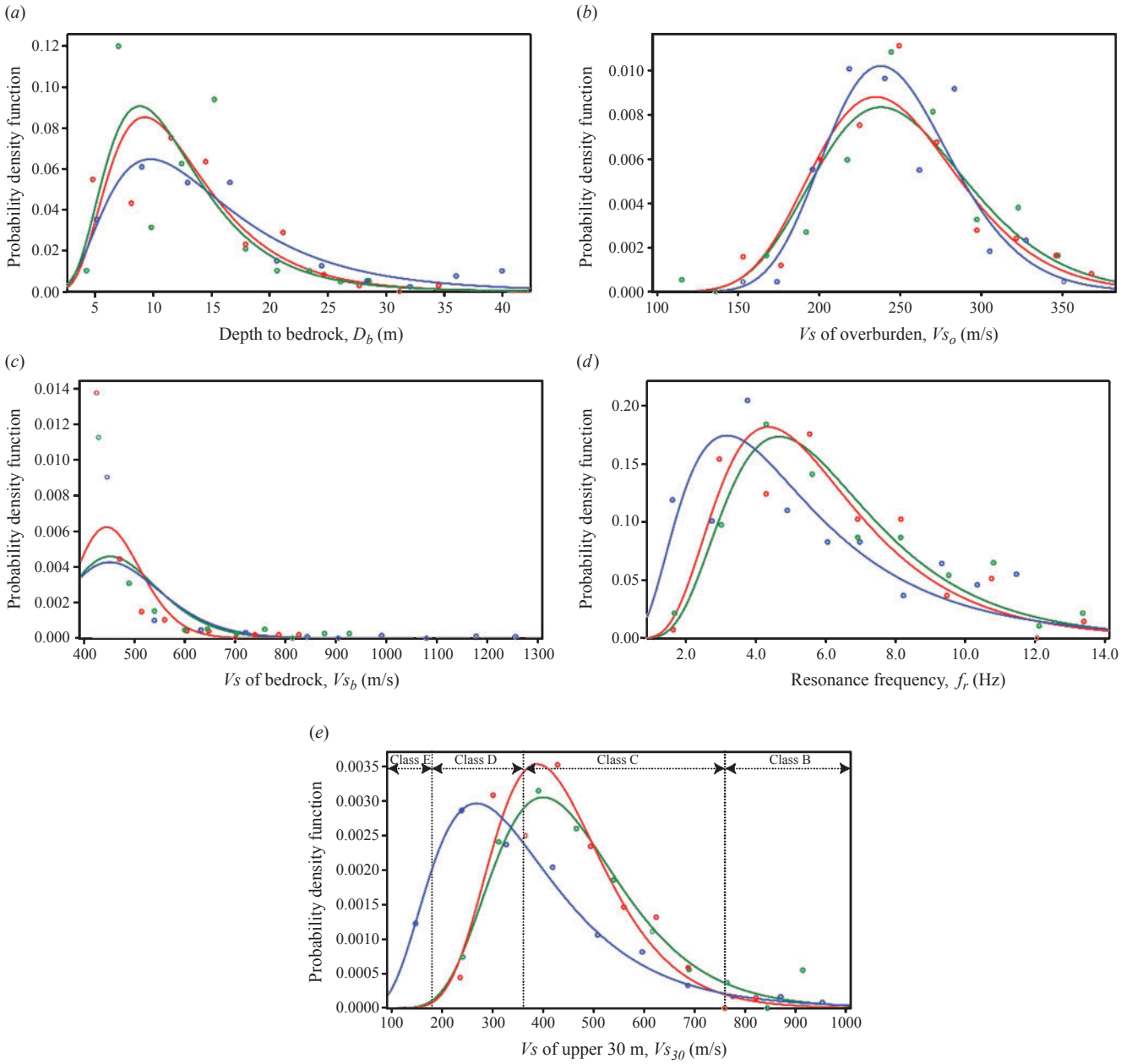

Fig. 2. Lognormal distributions (circles) and probability density functions (lines) of (*a*) depth to the bedrock (D_b), (*b*) Vs of the overburden (Vs_o), (*c*) Vs of the bedrock (Vs_b), (*d*) resonance frequency (f_r) and (*e*) Vs of upper 30 m depth (Vs_{30}), for Chuncheon (green), Wonju (red) and Gangneung (blue), respectively. The National Earthquake Hazards Reduction Program (NEHRP) seismic site classes (FEMA, 1995) are overlain on the Vs_{30} distribution plot (*e*).

clearly show that the probability of lower f_r values (<4 Hz) in Gangneung ($\overline{f_r} = 5.5 \pm 3.6$ Hz) is greater than in Chuncheon ($\overline{f_r} = 6.3 \pm 3.0$ Hz) and Wonju ($\overline{f_r} = 5.9 \pm 2.8$ Hz). This indicates greater vulnerability to seismic amplification in Gangneung.

In general, the computed $\overline{f_r}$ values for the three cities were slightly less than the average value of 6.6 ± 8.4 Hz which was previously estimated using data at 72 sites (Sun et al., 2007). However, our estimated $\overline{f_r}$ were much greater than the fundamental frequencies obtained largely by the horizontal-to-vertical spectral ratio method of ambient seismic noise recorded at 126 seismic stations in Italy (2.9 ± 2.2 Hz; Luzi et al., 2011); 35 sites in Kissamos, Greece (2.1 ± 2.5 Hz; Moisidi et al., 2015); and 28 sites in Switzerland (2.0 ± 2.3 Hz; Michel et al., 2014). The difference in geology, sampling density, and the methodology used may be responsible for the discrepancy in $\overline{f_r}$.

Vs of the top 30 m depth layer (Vs_{30})

Vs_{30} values were calculated at 72, 105 and 136 sites in Chuncheon, Wonju and Gangneung, respectively, using the following relationship (Borcherdt, 1994):

$$Vs_{30} = \frac{30}{\sum_{i=1}^{n} \frac{D_i}{V_{s_i}}}, \tag{7}$$

where D_i and S_i indicate the estimated thickness and Vs of the *i-th* layer, respectively (Table 1).

The estimated average Vs_{30} ($\overline{Vs_{30}}$) in Chuncheon was 462 ± 154 m/s, which is 15% greater than the previous estimate in Jung and Kim (2014). This updated estimation has been improved mainly by including supplementary data from high-altitude areas where samples were scarce. In the agricultural, downtown, forest and bare ground areas, the $\overline{Vs_{30}}$ values were

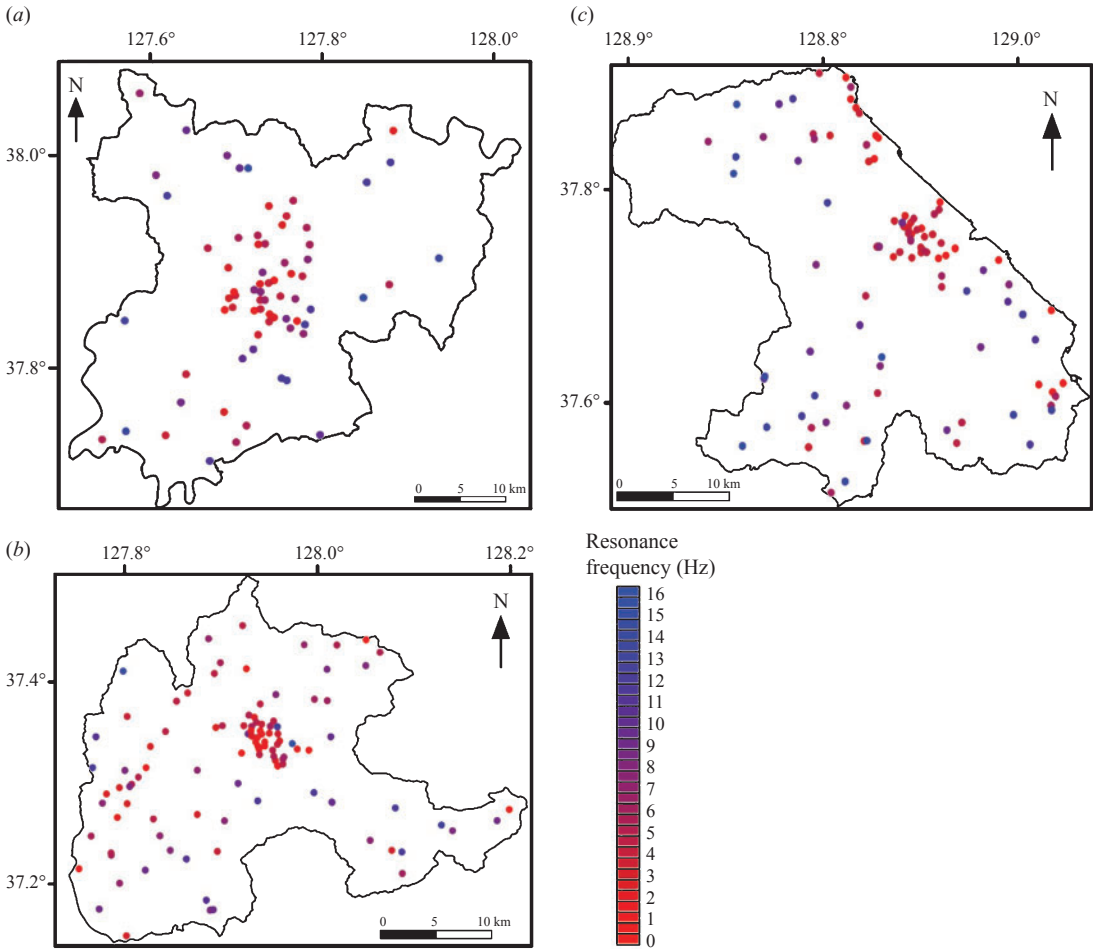

Fig. 3. Maps showing the variation in the resonance frequencies (f_r) in (*a*) Chuncheon, (*b*) Wonju and (*c*) Gangneung. The solid circles denote the corresponding f_r at that particular recording site.

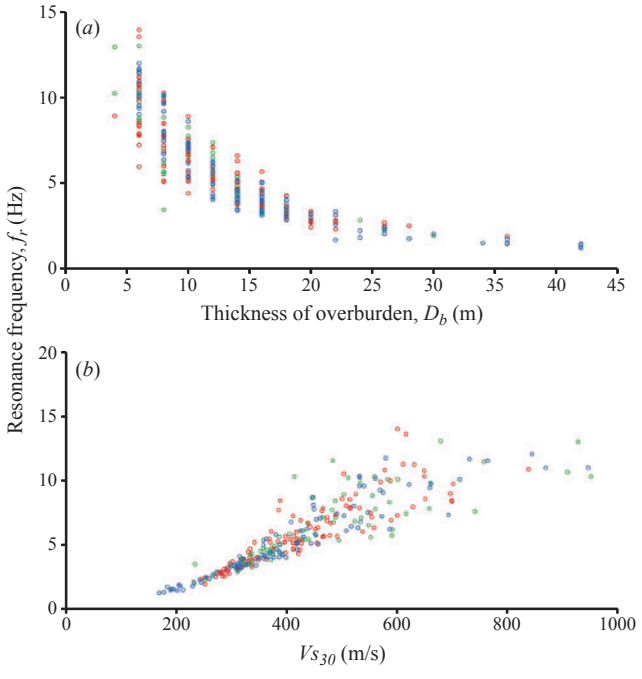

Fig. 4. Correlations of resonance frequency (f_r) with (*a*) depth to the bedrock (D_b), and (*b*) *Vs* of upper 30 m depth (Vs_{30}) in Chuncheon (green circles), Wonju (red circles) and Gangneung (blue circles), respectively.

447 ± 132, 388 ± 87, 642 ± 146 and 287 ± 52 m/s, respectively. The new estimate of $\overline{Vs_{30}}$ of 436 ± 125 m/s in Wonju is 4% larger than the previous estimate (Kim et al., 2014). Here, the $\overline{Vs_{30}}$ values were 449 ± 136, 390 ± 103 and 528 ± 92 m/s in the agricultural, downtown and forest areas, respectively. The $\overline{Vs_{30}}$ in Chuncheon and Wonju were comparable to the 460 ± 244 m/s determined by seismic tests at 72 sites in Korea (Sun et al., 2007). The $\overline{Vs_{30}}$ in Gangneung was estimated to be 364 ± 169 m/s in our previous study (Ali and Kim, 2016), while here the $\overline{Vs_{30}}$ values were 302 ± 153, 314 ± 102 and 424 ± 182 m/s in the agricultural, downtown and forest areas, respectively. These $\overline{Vs_{30}}$ values were lower than those estimated in Chuncheon and Wonju, and previous nationwide data (Sun et al., 2007). The lower $\overline{Vs_{30}}$ in Gangneung may be due to deeper bedrock depths. The Vs_{30} probability distribution curve (Figure 2*e*) for Gangneung ($\overline{Vs_{30}} = 364 \pm 174$ m/s) lies in a region of values lower than the respective curves for Chuncheon ($\overline{Vs_{30}} = 462 \pm 148$ m/s) and Wonju ($\overline{Vs_{30}} = 436 \pm 125$ m/s). The areas under the *Vs* probability curve less than or equal to 360 m/s (Class D) and 180 m/s (class E) thresholds are ~33% and 15%, respectively.

The $\overline{Vs_{30}}$ for all three cities were estimated to be 411 ± 157 m/s, with $\overline{Vs_{30}}$ values of 401 ± 155, 364 ± 106, 471 ± 182 and 287 ± 52 m/s in the agricultural, downtown, forest and bare ground areas, respectively. The $\overline{Vs_{30}}$ values were generally in a reasonable range compared to data for 52 sites in Parkfield, the United States (371 ± 142 m/s; Thompson et al., 2010); 44 sites in north-western Turkey (409 ± 119 m/s;

Karagoz et al., 2015); 126 sites in Italy (509 ± 253 m/s; Luzi et al., 2011); and 50 sites in Australia (569 ± 367 m/s; Kayen et al., 2015).

To verify Vs_{30} as a benchmark for seismic site conditions, correlation coefficients with f_r were examined (Figure 4*b*). The r values were estimated to be 0.82, 0.87 and 0.92 for Chuncheon, Wonju and Gangneung, respectively. The good correlations indicate that Vs_{30} has sufficient predictive power to assess seismic amplification risks when information for f_r and D_b is unavailable.

Correlation of Vs_{30} with elevation and topographic slope

The linear correlations of Vs_{30} with topographic slope and elevation were examined to find appropriate proxies for site conditions. To determine the optimum pixel sizes for the correlations, linear regression analyses of Vs_{30} were performed with the proxies on square pixels of 30, 100, 200, 277, 300, 400, 500 and 1000 m digital elevation models. For this range of pixel sizes, the r values of Vs_{30} with the elevation were in the ranges of 0.46–0.56, 0.43–0.49 and 0.54–0.57 for Chuncheon, Wonju and Gangneung, respectively (Figure 5*a*), while the r values of Vs_{30} with the topographic slope ranged from 0.17 to 0.39, 0.38 to 0.48 and 0.55 to 0.73, respectively (Figure 5*b*).

Although elevation is more strongly correlated with Vs_{30} than topographic slope, the former proxy is less sensitive to pixel size, with the range of r values being three times larger for the latter proxy than the former (Figure 5). Accordingly, the optimum pixel sizes were determined based on the topographic slope, and were 100, 200 and 277 m for Chuncheon, Wonju and Gangneung, respectively (Figure 5). These pixel sizes are less than 1 km, which was the value previously adopted for Chuncheon in Jung and Kim (2014) and Wonju in Kim et al. (2014). This may be due to additional recordings in high-altitude areas with variable topographic slope. The pixel sizes used in this study were at an intermediate scale between the 30 m previously adopted for the Santiago de Chile Basin (Pilz et al., 2010) and 1 km applied in the United States, Taiwan, Italy and Australia (Wald and Allen, 2007).

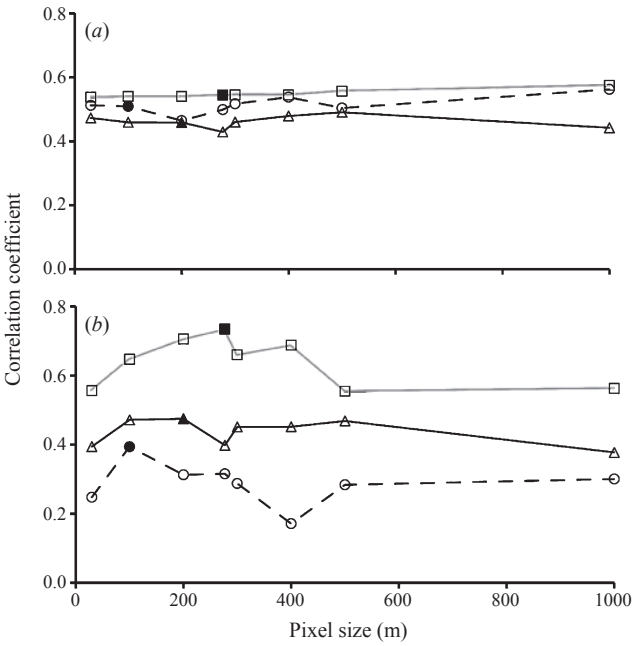

Fig. 5. Correlations of Vs of upper 30 m depth (Vs_{30}) with (*a*) elevation and (*b*) topographic slope at various pixel sizes in Chuncheon (circles on dashed line), Wonju (triangles on solid black line) and Gangneung (squares on solid grey line), respectively. The filled symbols represent the particular pixel size used for the multiple regression.

The optimum coefficients were determined for each city to enable the calculation of Vs_{30} in the multiple regression analyses (Figure 6):

$$Vs_{30} = A + BE_l + CT_s, \quad (8)$$

where A, B, and C are coefficients that must be estimated, and the proxies E_l and T_s represent the elevation and topographic slope at a specific sites, respectively. Before determining the coefficients for each city (Table 2), four outliers were removed from the 72 estimated values of Vs_{30} in Chuncheon, and three outliers were removed from the 105 estimates in Wonju. The standard errors (SEs) of the regressions were 117, 104 and 110 m/s for Chuncheon, Wonju,and Gangneung, respectively. The relatively large SE values indicate that proxy-based empirical relationships can only be applied regionally for the purpose of perspective. The mean absolute errors between the proxy-based Vs_{30} and the Vs_{30} derived from the inverted Vs profiles were

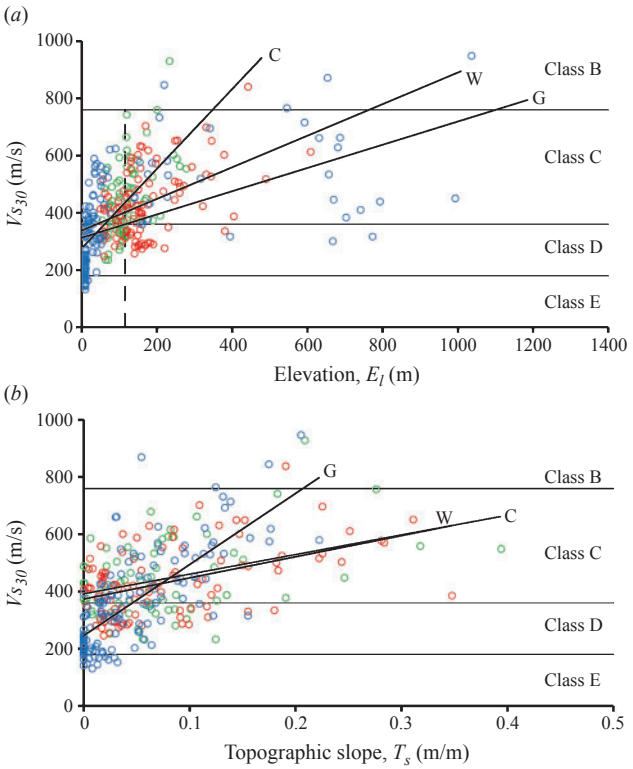

Fig. 6. Computed Vs of upper 30 m depth (Vs_{30}) versus (*a*) elevation and (*b*) topographic slope for Chuncheon (green circles; 'C'), Wonju (red circles; 'W') and Gangneung (blue circles; 'G'), with the corresponding linear regression lines labelled by C, W and G, respectively. The vertical dashed line in (*a*) indicates the Vs_{30} corresponding to the boundaries between classes C and D. Horizontal lines of Vs_{30} demarcating the site classes are also superimposed.

Table 2. Coefficients of the linear regression in Equation 8 for the major cities in Gangwon Province, Korea.

Coefficients	Chuncheon	Wonju	Gangneung
A	288	342	243
B	1.24	0.31	0.17
C	78	473	2090

87 ± 60, 82 ± 62 and 85 ± 68 m/s at recording stations in Chuncheon, Wonju and Gangneung, respectively.

Seismic microzonation

Because the spatial density of the recording sites was not high enough to construct accurate microzonation maps, a proxy-based Vs_{30} was determined at the centre of regularly spaced grids using Equation 8 with the derived coefficients (Table 2). As determined in the previous section, the lengths of the sides of the square grids were fixed to 100, 200 and 277 m for Chuncheon, Wonju and Gangneung, respectively.

The resulting microzonation maps for the three major cities based on the NEHRP site classification displayed strong correlations with the topographic data (Figure 7). The ground primarily consisted of classes B (31%), C (67%) and D (1%), with a smaller proportion of A (< 1%) in Chuncheon (Figure 7*a*). Mainly due to its high elevation (50 to 608 m; Figure 6*a*) and topographic slope (0.08 to 0.31 m/m; Figure 6*b*), most of the ground in Wonju was classified in class C (97%), with a small amount in B (2%) and a very small amount in class D (< 1%). Based on previous analyses of Vs_{30} (Ali and Kim, 2016), the ground in Gangneung consists of classes B (37%), C (45%) and D (18%).

The site classification based on the proxy-based Vs_{30} may be misleading at a small scale. Although no class E was indicated from the above analyses, the Vs_{30} values derived from the Rayleigh-wave dispersion curves recorded at 13 sites in Gangneung were less than 180 m/s, which is the boundary between classes D and E (Figure 6*a*). This discordance arose from the wide range of inverted Vs_{30} values at low altitudes. The altitude corresponding to a Vs_{30} of 180 m/s on the regressed line was 115 m. This strongly indicates that areas in class E should exist in the city. Simply by assuming the normal distribution of Vs_{30}, 16% of the area determined as class D based on the proxy-based Vs_{30} is probably in class E. Both the high proportion of class D category surface cover and the existence of an inverted Vs_{30} less than 180 m/s indicate that ground amplification and soil liquefaction risks during earthquakes will be higher in Gangneung than in the other two cities

Overall, using the proxy-based Vs_{30} at 150 507 sites revealed that the three cities could mainly be classified into surface cover of classes B (27%), C (69%) and D (3%), with minor proportions of A (< 1%). The downtown and agricultural areas that were mostly located at low-altitudes, and were composed of Quaternary alluvium and fluvial terrace deposits, were categorised as classes C and D. This suggests that the ground amplification risks in these areas are likely to be greater than the in the high-altitude forest areas of site classes A and B.

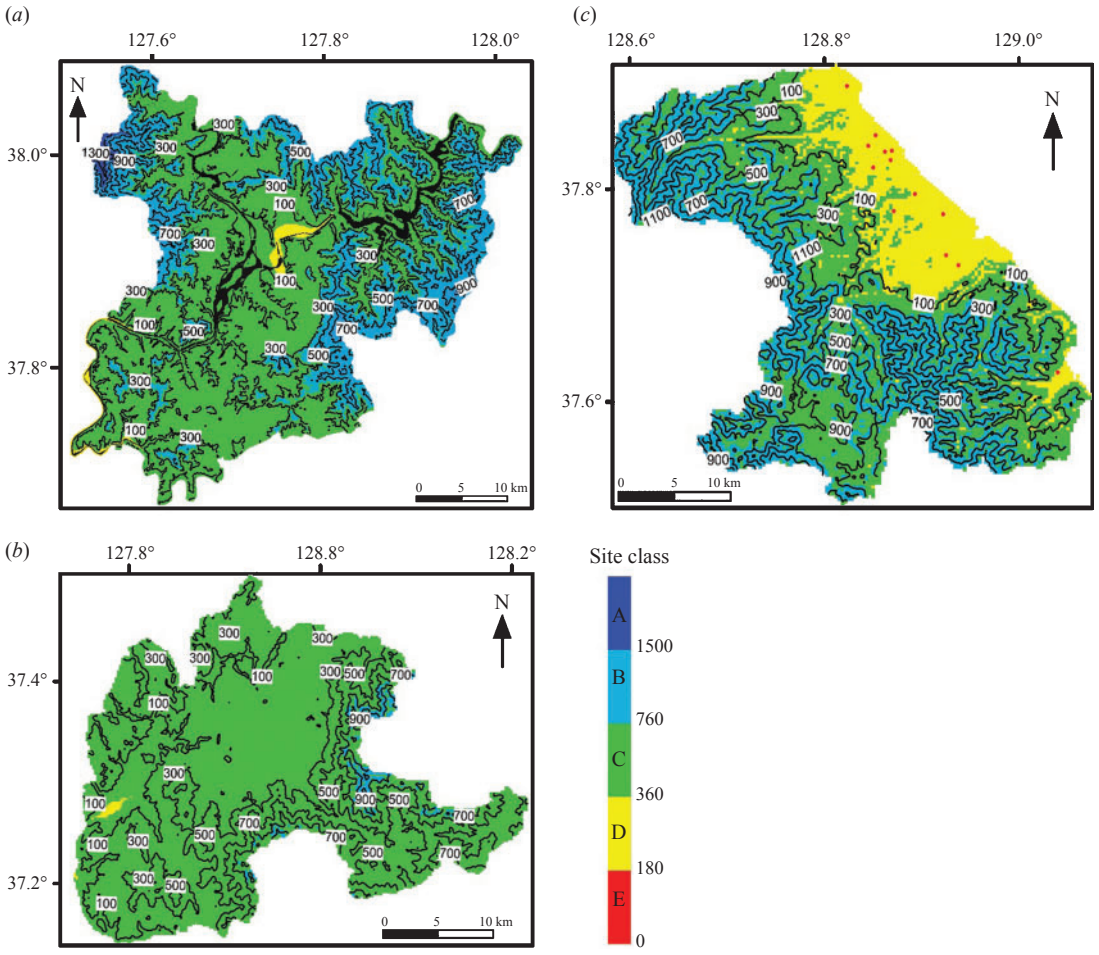

Fig. 7. Seismic microzonation maps based on the 1994 seismic site classes of the National Earthquake Hazards Reduction Program (NEHRP) (FEMA, 1995) for (*a*) Chuncheon, (*b*) Wonju and (*c*) Gangneung. The recording sites where the *Vs* of upper 30 m depth (Vs_{30}), derived from the Rayleigh-wave dispersion curves, were less than 180 m/s are indicated with red circles. Contour lines at intervals of 200 m are superimposed on the microzonation maps and illustrate the coherence between the elevation and seismic site classes.

Conclusions

In three major cities (Chuncheon, Wonju, and Gangneung) in Gangwon Province, Korea, the $\overline{D_b}$ was 13 ± 7, $\overline{Vs_b}$ was 472 ± 109 m/s, $\overline{Vs_o}$was 248 ± 44 m/s, $\overline{Vs_{30}}$ was 411 ± 157 m/s and $\overline{f_r}$ was 5.8 ± 2.8 Hz. With regard to land cover, the estimated Vs_{30} was lowest for the bare ground (287 ± 52 m/s), followed by the downtown (364 ± 106 m/s), agricultural (401 ± 155 m/s) and forest regions (471 ± 182 m/s). The strong correlations between Vs_{30} and f_r indicate that Vs_{30} has sufficient predictive power to evaluate seismic amplification risks when information for f_r and D_b is unavailable.

The microzonation maps based on the proxy-based Vs_{30} at 150 507 sites revealed that the surface cover of the three cities could mainly be categorised into NEHRP site classes B (27%), C (69%), and D (3%), with minor proportions of A (<1%). Most areas (97%) in Wonju were within class C, while more than one-third of Chuncheon and Gangneung were in class B. The downtown and agricultural areas, with low f_r values were categorised as classes C and D, which indicates a greater risk of ground amplification than the high-altitude forest areas of site classes A and B. These maps, together with information regarding the f_r, can effectively be used in seismic risk assessment, urban planning and disaster management in these major cities.

Of the cities studied here, Gangneung had the least Vs_o, Vs_{30} and f_r, and the greatest D_b. The Vs_{30} profiles derived at 13 sites in Gangneung were less than 180 m/s, although no area was estimated to be in class E using the proxy-based Vs_{30}. This indicates that of the cities studied here, Gangneung has the highest susceptibility to ground shaking during large earthquakes.

Acknowledgements

This research was supported by the Korea Meteorological Administration Research and Development Program under Grant CATER 2012–8040.

References

Aki, K., 1957, Space and time spectra of stationary stochastic waves, with special reference to microtremors: *Bulletin of Earthquake Research Institute*, **35**, 415–456.

Ali, A., 2016, Seismic site conditions and microzonation of the three major cities in Gangwon Province, Korea: Ph.D. thesis, Kangwon National University.

Ali, A., and Kim, K. Y., 2016, Seismic site conditions in Gangneung, Korea, based on Rayleigh-wave dispersion curves and topographic data: *Geosciences Journal*, **20**, 781–791. doi:10.1007/s12303-016-0013-1

Allen, T. I., and Wald, D. J., 2009, On the use of high-resolution topographic data as a proxy for seismic site conditions (Vs30): *Bulletin of the Seismological Society of America*, **99**, 935–943. doi:10.1785/0120080255

Anbazhagan, P., and Sitharam, T. G., 2009, Spatial variability of the depth of weathered and engineering bedrock using multichannel analysis of surface wave method: *Pure and Applied Geophysics*, **166**, 409–428. doi:10.1007/s00024-009-0450-0

Anbazhagan, P., Sheikh, M., and Parihar, A., 2013, Influence of rock depth on seismic site classification for shallow bedrock regions: *Natural Hazards Review*, **14**, 108–121. doi:10.1061/(ASCE)NH.1527-6996.0000088

Annaka, T., Yamazaki, F., and Katahira, F., 1997, A proposal of an attenuation model for peak ground motions and 5% damped acceleration response spectra based on the JMA-87 type strong motion accelerograms: *Proceedings of 24th JSCE Earthquake Engineering Symposium*, 161–164 [in Japanese].

Ansal, A., and Tönük, G., 2007, Source and site factors in microzonation, *in* K. D. Pitaliks, ed., *Earthquake geotechnical engineering: fourth international conference on earthquake geotechnical engineering-invited lectures*: Springer, 73–92.

Asten, M. W., 2006, On bias and noise in passive seismic data from finite circular array data processed using SPAC methods: *Geophysics*, **71**, V153–V162. doi:10.1190/1.2345054

Boatwright, J., Fletcher, J. B., and Fumal, T. E., 1991, A general inversion scheme for source, site, and propagation characteristics using multiply recorded sets of moderate-sized earthquakes: *Bulletin of the Seismological Society of America*, **81**, 1754–1782.

Borcherdt, R. D., 1970, Effects of local geology on ground motion near San Francisco Bay: *Bulletin of the Seismological Society of America*, **60**, 29–61.

Borcherdt, R. D., 1994, Estimates of site-dependent response spectra for design (methodology and justification): *Earthquake Spectra*, **10**, 617–653. doi:10.1193/1.1585791

Building Seismic Safety Council (BSSC), 1997, NEHRP recommended provisions for new buildings and other structures, Part 1 – Provisions, report no. FEMA-302, Federal Emergency Management Agency, Washington, D.C., 337 p.

Building Seismic Safety Council (BSSC), 2003, NEHRP recommended provisions for new buildings and other structures, Part 1 – Provisions, report no. FEMA-450, Federal Emergency Management Agency, Washington, D.C., 339 p.

Chiou, B., Darragh, R., Gregor, N., and Silva, W., 2008, NGA project strong-motion database: *Earthquake Spectra*, **24**, 23–44. doi:10.1193/1.2894831

Chiu, J.-M., and Kim, S. G., 2004, Estimation of regional seismic hazard in the Korean peninsula using historical earthquake data between A.D. 2 and 1995: *Bulletin of the Seismological Society of America*, **94**, 269–284. doi:10.1785/0120010256

Federal Emergency Management Agency (FEMA), 1995, 1994 NEHRP Recommended Provisions for Seismic Regulations of New Buildings; Part I, Provisions, FEMA 222A, National Earthquake Hazard Reduction Program, Federal Emergency Management Agency, Washington, D.C., 271 p.

Haskell, N. A., 1953, The dispersion of surface waves on multilayered media: *Bulletin of the Seismological Society of America*, **43**, 17–34.

Haskell, N. A., 1960, Crustal reflection of plane Sh waves: *Journal of Geophysical Research*, **65**, 4147–4150. doi:10.1029/JZ065i012p04147

Hayashi, K., Inazaki, T., and Suzuki, H., 2006, Buried incised-channels delineation using microtremor array measurements at Soka and Misato Cities in Saitama prefecture: *Butsuri Tansa*, **57**, 309–325 [in Japanese with an English abstract].

Houng, S. E., and Hong, T. K., 2013, Probabilistic analysis of the Korean historical earthquake records: *Bulletin of the Seismological Society of America*, **103**, 2782–2796. doi:10.1785/0120120318

International Code Council (ICC), 1997, 1997 Uniform Building Code: Volume 2 – Structural Engineering Design Provisions, International Conference of Building Officials, Whittier, California, 492 p.

International Code Council (ICC), 2000, 2000 International Building Code (IBC), 2000, International Code Council, Country Club Hills, Illinois, USA, 756 p.

International Code Council (ICC), 2003, 2003 International Building Code (IBC), International Code Council, Falls Church, Virginia, USA, 660 p.

International Institute of Seismology and Earthquake Engineering (IISEE), 2016, Building Research Institute, Japan. [Web document]. Available at http://iisee.kenken.go.jp (accessed 9 March 2016).

Iwata, T., and Irikura, K., 1988, Source parameters of the 1983 Japan Sea earthquake sequence: *Journal of Physics of the Earth*, **36**, 155–184. doi:10.4294/jpe1952.36.155

Jo, N., and Baag, C.-E., 2007, The 20 January 2007, MW 4.5, Odaesan, Korea, earthquake: *Geosciences Journal*, **11**, 51–58. doi:10.1007/BF02910380

Jung, J., and Kim, K. Y., 2014, Site characterization using shear-wave velocities inverted from Rayleigh-wave dispersion curves in Chuncheon, Korea: *Geophysics and Geophysical Exploration*, **17**, 1–10 [in Korean with an English abstract]. doi:10.7582/GGE.2014.17.1.001

Kang, T. S., and Baag, C. E., 2004, The 29 May 2004, MW = 5.1, offshore Uljin earthquake, Korea: *Geosciences Journal*, **8**, 115–123. doi:10.1007/BF02910189

Karagoz, O., Chimoto, K., Citak, S., Ozel, O., Yamanaka, H., and Hatayama, K., 2015, Estimation of shallow S-wave velocity structure and site response characteristics by microtremor array measurements in

Tekirdag region, NW Turkey: *Earth, Planets, and Space*, **67**, 176. doi:10.1186/s40623-015-0320-1

Kayen, R. E., Carkin, B. A., Allen, T., Collins, C., McPherson, A., and Minasian, D., 2015, Shear-wave velocity and site-amplification factors for 50 Australian sites determined by the spectral analysis of surface waves method: U.S. Geological Survey Open-File Report 2014–1264, Reston, U.S.A., 118 p.

Keçeli, A., 2012, Soil parameters which can be determined with seismic velocities: *Jeofizik*, **16**, 17–29.

Kihm, Y. H., and Hwang, J. H., 2011, Geological report of Gangneung-Jumunjin sheets (1 : 50,000): Korea Institute of Geosciences and Mineral Resources, Daejeon, Korea, 75 p.

Kim, C., Ali, A., and Kim, K. Y., 2014, Site characterization using shear-wave velocities inverted from Rayleigh-wave dispersion curves in Wonju, Korea: *Geophysics and Geophysical Exploration*, **17**, 11–20 [in Korean with an English abstract]. doi:10.7582/GGE.2014.17.1.011

Kim, K. Y., Ali, A., Jung, J., and Kim, C., 2015, Site classification for seismic-hazard assessment using geophysical methods. CATER 2012–8040, Korea Meteorological Administration, Seoul, 131 p. [in Korean with an English abstract].

Korean Ministry of Environment (KME), 2014, *Land Cover Map* (*2008–2010*) [Web document]. Available at http://egis.me.go.kr (accessed 7 January 2014).

Korean Rural Community Corporation (KRC), 2014, *Rural Groundwater Net* [Web document]. Available at https://www.groundwater.or.kr (accessed 3 January 2014).

Korean Statistical Information Service (KOSIS), 2015, *Statistical Database*, Statistics Korea [Web document]. Available at http://kosis.kr (accessed 20 December 2015).

Lee, D. S., Lee, H. T., Nam, K. S., and Yang, S. Y., 1974, Explanatory text of the geological map of Chuncheon sheet (1 : 50,000), Chuncheon Sheet 6727–IV: Korea Institute of Geosciences and Mineral Resources, Daejeon, Korea, 47 p.

Lermo, J., and Chávez-García, F. J., 1993, Site effect evaluation using spectral ratios with only one station: *Bulletin of the Seismological Society of America*, **83**, 1574–1594.

Ling, S., and Okada, H., 1993, An extended use of the spatial autocorrelation method for the estimation of geologic structure using microtremors: *Proceedings of the 89th SEGJ Conference*, 44–49 [in Japanese].

Luzi, L., Puglia, R., Pacor, F., Gallipoli, M. R., Bindi, D., and Mucciarelli, M., 2011, Proposal for a soil classification based on parameters alternative or complementary to Vs, 30: *Bulletin of Earthquake Engineering*, **9**, 1877–1898. doi:10.1007/s10518-011-9274-2

Marquardt, D., 1963, An algorithm for least square estimation of nonlinear parameters: *Journal of the Society for Industrial and Applied Mathematics*, **11**, 431–441. doi:10.1137/0111030

Michel, C., Edwards, B., Poggi, V., Burjánek, J., Roten, D., Cauzzi, C., and Fäh, D., 2014, Assessment of site effects in alpine regions through systematic site characterization of seismic stations: *Bulletin of the Seismological Society of America*, **104**, 2809–2826. doi:10.1785/0120140097

Miller, R. D., Xia, J., Park, C. B., and Ivanov, J. M., 1999, Multichannel analysis of surface waves to map bedrock: *The Leading Edge*, **18**, 1392–1396. doi:10.1190/1.1438226

Ministry of Construction and Transportation (MOCT), 1997, Korean Seismic Design Standard, Ministry of Construction and Transportation, Seoul, Korea, 492 p. [in Korean].

Ministry of Land Infrastructure and Transportation (MOLIT), 2014, *Geotechnical Information Portal System*, Ministry of Land, Infrastructure and Transportation, Sejong, Korea [Web document]. Available at http://www.geoinfo.or.kr (accessed 4 January 2014).

Moisidi, M., Vallianatos, F., Kershaw, S., and Collins, P., 2015, Seismic site characterization of the Kastelli (Kissamos) basin in northwest Crete (Greece): assessments using ambient noise recordings: *Bulletin of Earthquake Engineering*, **13**, 725–753. doi:10.1007/s10518-014-9647-4

Nakamura, Y., 1988, On the urgent earthquake detection and alarm system (UrEDAS): *Proceedings of Ninth World Conference in Earthquake Engineering*, Tokyo, Japan, 485–494.

Okada, H., 2003, *The microtremor survey method* (Geophysical Monograph Series Number 12): Society of Exploration Geophysicists.

Park, B. K., Chang, H. W., and Woo, Y. K., 1989, Geological map of Korea; 1 : 50,000 Wonju: Korea Institute of Energy and Resources, Seoul, Korea, 37 p.

Pilz, M., Parolai, S., Picozzi, M., Wang, R., Leyton, F., Campos, J., and Zschau, J., 2010, Shear wave velocity model of the Santiago de Chile basin derived from ambient noise measurements: a comparison of proxies for seismic site conditions and amplification: *Geophysical Journal International*, **182**, 355–367.

Pugin, A. J. M., Pullan, S. E., and Hunter, J. A., 2013, Shear-wave high-resolution seismic reflection in Ottawa and Quebec City, Canada: *The Leading Edge*, **32**, 250–255. doi:10.1190/tle32030250.1

Romero, S., and Rix, G. J., 2001, Regional variations in near-surface shear wave velocity in the greater Memphis area: *Engineering Geology*, **62**, 137–158. doi:10.1016/S0013-7952(01)00059-X

Scasserra, G., Stewart, J. P., Kayen, R. E., and Lanzo, G., 2009, Database for earthquake strong motion studies in Italy: *Journal of Earthquake Engineering*, **13**, 852–881. doi:10.1080/13632460802566997

Schwab, F., 1970, Surface-wave dispersion computations, Knopoff's method: *Bulletin of the Seismological Society of America*, **60**, 1491–1520.

Seyhan, E., Stewart, J. P., Ancheta, T. D., Darragh, R. B., and Graves, R. W., 2014, NGA-West2 site database: *Earthquake Spectra*, **30**, 1007–1024. doi:10.1193/062913EQS180M

Steidl, J. H., 2000, Site response in southern California for probabilistic seismic hazard analysis: *Bulletin of the Seismological Society of America*, **90**, S149–S169. doi:10.1785/0120000504

Sun, C. G., Chung, C. K., and Kim, D. S., 2007, Determination of mean shear wave velocity to the depth of 30 m based on shallow shear wave velocity profile: *Journal of the Earthquake Engineering Society of Korea*, **11**, 45–57 [in Korean with an English abstract]. doi:10.5000/EESK.2007.11.1.045

Sun, C. G., Han, J. T., and Cho, W, 2012, Representative shear wave velocity of geotechnical layers by synthesizing in-situ seismic test data in Korea: *The Journal of Engineering Geology*, **22**, 293–307. doi:10.9720/kseg.2012.3.293 [in Korean with an English abstract]

Sun, C.-G., Kim, B.-H., Park, K.-H., and Chung, C.-K., 2015, Geotechnical comparison of weathering degree and shear wave velocity in the decomposed granite layer in Hongseong, South Korea: *Environmental Earth Sciences*, **74**, 6901–6917. doi:10.1007/s12665-015-4692-0

Thompson, E. M., and Wald, D. J., 2012, Developing Vs30 site-condition maps by combining observations with geologic and topographic constraints: 15th World Conference on Earthquake Engineering (WCEE), Lisbon, Portugal, 24–28 September, 9 pp.

Thompson, E. M., Kayen, R. E., Carkin, B., and Tanaka, H., 2010, Surface-wave site characterization at 52 strong-motion recording stations affected by the Parkfield, California, M 6.0 earthquake of 28 September 2004: U.S. Geological Survey Open-File Report 2010–1168, Reston, U.S.A., 117 p.

Thomson, W. T., 1950, Transmission of elastic waves through a stratified solid, analytical results: *Journal of Applied Physics*, **21**, 89–93. doi:10.1063/1.1699629

Tokeshi, K., Harutoonian, P., Leo, C. J., and Liyanapathirana, S., 2013, Use of surface waves for geotechnical engineering applications in western Sydney: *Advances in Geosciences*, **35**, 37–44. doi:10.5194/adgeo-35-37-2013

Wald, D. J., and Allen, T. I., 2007, Topographic slope as a proxy for seismic site conditions and amplification: *Bulletin of the Seismological Society of America*, **97**, 1379–1395. doi:10.1785/0120060267

Wills, C. J., and Clahan, K. B., 2006, Developing a map of geologically defined site-condition categories for California: *Bulletin of the Seismological Society of America*, **96**, 1483–1501. doi:10.1785/0120050179

Xia, J., Miller, R. D., and Park, C. B., 1999, Estimation of near-surface shear-wave velocity by inversion of Rayleigh waves: *Geophysics*, **64**, 691–700. doi:10.1190/1.1444578